

# Tars removal by non-thermal plasma and plasma catalysis

Richard Cimerman<sup>✉</sup>, Diana Račková and Karol Hensel<sup>✉</sup>

Faculty of Mathematics, Physics and Informatics, Comenius University, Mlynská Dolina F2, 842 48, Bratislava, Slovakia

E-mail: [cimerman@fmph.uniba.sk](mailto:cimerman@fmph.uniba.sk)

Received 5 February 2018, revised 15 May 2018

Accepted for publication 23 May 2018

Published 13 June 2018



CrossMark

## Abstract

The gasification of a fuel or biomass is an industrial process that is utilized for synthesis gas (syngas) production. The syngas can be used to generate electricity, but after gasification it is often polluted with tars and various other pollutants. Therefore, the syngas must be cleaned before further use. The objective of this paper was to investigate the potential of removing the tars by non-thermal plasma generated by atmospheric pressure dielectric barrier discharge in combination with various packing materials ( $\text{TiO}_2$ ,  $\text{Pt}/\gamma\text{-Al}_2\text{O}_3$ ,  $\gamma\text{-Al}_2\text{O}_3$ , glass beads). Naphthalene was used as a model polyaromatic tar compound. The effect of discharge power, carrier gas and packing material on naphthalene removal was investigated and gaseous and solid by-products were analysed by means of FTIR spectrometry. In ambient air, a naphthalene removal efficiency of 88% and 40% was achieved for  $320 \text{ J l}^{-1}$  with and without the catalyst, respectively. The maximum removal efficiency of almost 100% was observed with a  $\text{TiO}_2$  catalyst and oxygen carrier gas.  $\text{CO}$ ,  $\text{CO}_2$ ,  $\text{H}_2\text{O}$  and  $\text{HCOOH}$  were identified among the products, as well as more complex compounds, such as 1,4-naphthoquinone and phthalic anhydride.

Keywords: non-thermal plasma, dielectric barrier discharge, plasma catalysis, naphthalene removal,  $\text{TiO}_2$ ,  $\text{Pt}/\gamma\text{-Al}_2\text{O}_3$

(Some figures may appear in colour only in the online journal)

## 1. Introduction

Growing global energy demand and an aversion against the use of fossil fuels on environmental grounds have led to interest in alternative technologies and processes for heat and electricity production. Among the alternative energy sources, biomass and municipal solid waste have a special position due to their wide availability. Biomass is the oldest carbon neutral renewable energy source, while municipal solid waste offers the advantage of simultaneous energy recovery and reduction of waste volume otherwise destined for landfills [1, 2]. In order to generate electricity, biomass and waste can be either combusted or efficiently gasified into a biomass derived fuel gas. This gas, also called producer gas or synthesis gas (syngas), is a mixture of carbon monoxide ( $\text{CO}$ ), hydrogen ( $\text{H}_2$ ), carbon dioxide ( $\text{CO}_2$ ) and methane ( $\text{CH}_4$ ), and possesses high energy potential. The chemical energy

contained in the syngas can be used directly to generate electricity using internal combustion gas turbines or engines, or transformed into chemicals, e.g. methanol, synthetic natural gas, etc [3]. In all industrial applications utilizing syngas, high quality and purity is required. However, the syngas produced by gasification often contains various pollutants, including particulate matter (fly ash and soot), tars, dioxins, furans, metal vapours, nitrogen and sulphur compounds, that disqualify it from further utilization. Among these pollutants, tar contaminants in particular are consistently associated with system malfunction and the corrosion of metal materials. The tars constrain the heating value of the fuel gas, block particle filters and pipelines, deactivate the catalysts and also have a negative effect on human health and the environment [4]. In general, tar compounds are a complex mixture of condensable hydrocarbons, including single-ring to multiple-ring aromatic compounds, along with other substituents [5]. They can be

classified according to their structure, chemical stability and reactivity, solubility or condensability. We divide them into five groups: GC-undetectable (very heavy tars), heterocyclic (e.g. phenols, pyridine), light aromatic (e.g. toluene, xylene), light polyaromatic (e.g. naphthalene, anthracene) and heavy polyaromatic (e.g. fluoranthene, pyrene) tars [4].

In the process of making syngas technologies technically and commercially feasible, tar removal represents a major challenge. Several commercial methods for tar removal exist—mechanical and physical methods, including cyclones, bag filters, wet scrubbers, electrostatic precipitators, etc. and thermal or catalytic cracking methods. The efficient decomposition of tars by thermal methods requires temperatures from 700 °C to 1250 °C, while catalytic methods require slightly lower temperatures from 550 °C to 900 °C [4]. The most commonly used technique is currently chemical catalysis. The role of the catalyst in the process is to lower the reaction activation energies for the desired chemical reactions. The catalyst activity leads to an increase of the chemical reaction rate and the improvement of the selectivity for the desired product. The ideal catalyst is expected to be chemically, mechanically and thermally stable. The most used and studied catalytic materials for tar removal are Ni-, Rh-, Pt-, Fe-, olivine-, dolomite- and zeolite-based catalysts [4–8]. Although thermal and catalytic methods provide high tar removal efficiencies, they also require an additional supply of heat. Moreover, catalyst lifetime is always a limiting factor due to catalyst deactivation or poisoning caused by its exposure to a range of chemical compounds and particulate matter, i.e. fly ash and soot.

Non-thermal plasma (NTP) processes have been studied extensively for many years in numerous environmental applications, especially for air and water pollution control [9, 10]. NTP can be generated by atmospheric pressure discharges, such as corona discharge, dielectric barrier discharge (DBD) or spark discharge, by applying sufficiently strong electric fields to the enclosed gas mixture, which initiate electron avalanche and streamer formation. Due to their light mass, the electrons in the gas are accelerated, gain high energies (1–10 eV) and are not in thermal equilibrium with the other particles (ions, neutrals). The collisions of high-energy electrons with bulk gas molecules ( $N_2$ ,  $O_2$ ,  $H_2O$ ) result in the formation of highly reactive short-lived species (e.g.  $\cdot O$ ,  $\cdot N$ ,  $\cdot OH$ ). These species, along with other reactive species ( $O_3$ ,  $N_2^*$ ,  $O_2^*$ ) in the highly reactive NTP, can subsequently react with gas pollutant molecules and decompose them by the processes of oxidation or reduction to harmless compounds. The removal of hydrocarbons, including volatile organic compounds (VOCs), by NTP has been investigated by many research groups, is well documented and has been discussed in several papers [11–15]. Benzene, toluene, trichloroethylene and formaldehyde are among the most commonly used target compounds. With respect to electric discharge as a source of NTP, DBD has typically been used due to its simplicity and scalability, and the availability of reliable, efficient and affordable power supplies [16].

NTP gas processing for hydrocarbon removal usually possesses decent removal efficiency, but unfortunately also has several disadvantages, such as the formation of undesirable

by-products and organic intermediates, the low selectivity of the chemical reactions and high energy consumption, which limit its practical use. To suppress or even overcome these disadvantages, a combination of NTP with catalysts seems to be a promising method that would allow us to utilize the individual benefits of the two techniques [17, 18]. The catalyst can be placed either behind the plasma zone (so-called plasma-assisted catalysis or post-plasma catalysis) or directly in the plasma zone (plasma-driven catalysis or in-plasma catalysis). The catalyst can be present as a coating or as a layer on the plasma reactor walls or electrodes, or it can take the form of beads, pellets, powder or granulates packed in the reactor volume [19]. Plasma catalysis might be characterized by synergistic effects that only occur for the combination of plasma with catalysis and not for plasma or catalysis alone [20]. Therefore, the combined effect of the plasma with the catalyst is usually stronger than the sum of their individual effects and results in the remarkable enhancement of the reactant removal and the yield of desired products, as well as the higher energy efficiency of the process [21]. These synergistic effects in plasma catalysis are a complex phenomenon and are the result of the mutual interplay between the various processes of plasma–catalyst interaction [22]. The plasma affects the catalyst via plasma-induced morphological, chemical and electronic changes in the catalyst, changes in surface adsorption processes, modification of the reaction pathways, lowering of activation barriers, thermal or light emission triggering photocatalysis, etc. In reverse, the presence of the catalyst affects the plasma via enhancement of the electric field near the catalyst surface that may result in a change of discharge mode, a change in the electron energy distribution, the formation of reactive species, etc [20, 22–24]. As a result, plasma catalysis is not only utilized in environmental applications, such as  $NO_x$ ,  $SO_x$  or VOC removal [11, 24–33], but also for various energy applications, e.g. fuel reforming and hydrogen generation [24, 33, 34].

Tar removal processes that employ NTP have been studied by several research groups in recent years. The majority of studies focused on NTP tar removal processes using pulsed [3, 5, 35–37] or DC corona discharge [38], DBD [39–41] or gliding arc discharge [42–48]. Pemen *et al* [3], Devi *et al* [5] and Nair *et al* [35, 36] used streamer corona discharge powered by a pulsed high voltage power supply and studied the effect of gas temperature (200 °C–500 °C), gas composition (various mixtures of synthetic syngas, including compounds such as  $CO$ ,  $CO_2$ ,  $H_2$ ,  $CH_4$ ,  $H_2O$  and  $N_2$ , and additives like Ar or air) and discharge energy density (up to 550 J l<sup>-1</sup>). In their works, naphthalene, toluene and phenol with initial concentrations in the range of 500–700 ppm were used as model tar compounds. They found that tar removal was mainly governed by oxidative processes mediated by O radicals generated by  $O_2$  or  $CO_2$  dissociation and in the presence of  $H_2O$  by a combination of both H and OH radicals formed by  $H_2O$  dissociation. The importance of the presence of  $O_2$  for naphthalene decomposition was also confirmed by Wu *et al* [39], who studied the effect of DBD in  $O_2/N_2$  mixtures with various  $O_2$  concentrations. Other works used DBD packed with glass beads with and without the addition of char particles in

syngas-like mixtures at 350 °C [40] or surface DBD in air-like mixtures at room temperature [41]. A tar decomposition process that employed gliding arc discharge was investigated on several surrogates of biomass tars—pyrene [42], toluene [43], naphthalene [44, 45] and toluene and naphthalene [46, 47] or benzene and naphthalene [48] mixtures. These works asserted the important role of OH radicals in tar decomposition processes, as formed by direct electron impacts with H<sub>2</sub>O and also via the interaction of electrically excited oxygen and nitrogen molecules with H<sub>2</sub>O.

Although tar removal by NTP is quite well documented, the removal of tar by a combination of NTP with catalysts in plasma catalytic systems has been investigated less frequently. Tar removal by plasma catalysis has only been reviewed in a few papers, with toluene being the most common target tar compound [49–51]. Tao *et al* [49] performed a comparative study of tar removal techniques and showed that plasma catalytic steam reforming over Ni/SiO<sub>2</sub> catalyst with pulsed NTP showed the greatest toluene removal and selectivity for syngas production. Liu *et al* [50] also investigated plasma catalytic steam reforming but over Ni/Al<sub>2</sub>O<sub>3</sub> catalyst with a coaxial DBD reactor. They found that coupling plasma with the catalyst not only enhanced the toluene removal and H<sub>2</sub> yield, but also significantly suppressed the formation of undesirable by-products in comparison with plasma processing alone. Liu *et al* [51] used Ni/Al<sub>2</sub>O<sub>3</sub> and Fe/Al<sub>2</sub>O<sub>3</sub> catalysts in a DBD reactor and showed that syngas was the dominant gaseous product of toluene decomposition. Toluene is one of the simplest aromatic tar compounds, but the tars produced by gasification are usually more complex and include many other light and heavy polyaromatic compounds. Therefore, the effect of plasma catalysis on polyaromatic compounds must also be investigated. As a model polyaromatic tar compound, naphthalene, as the simplest and the least toxic polycyclic aromatic hydrocarbon (PAH), is usually used. However, the number of studies related to its removal by plasma catalysis is very limited. Gao *et al* [52] studied a corona discharge radical shower system with/without MnO<sub>2</sub> catalyst coated on the negative electrode of the reactor in air-like mixtures. They found that the presence of the catalyst and humidity improved naphthalene decomposition. Nair [53] investigated the effect of pulsed corona discharge with  $\gamma$ -Al<sub>2</sub>O<sub>3</sub> catalyst at a temperature of 300 °C in dry reforming conditions (a mixture of N<sub>2</sub> + CO<sub>2</sub>) with/without CO added. The results showed that plasma catalysis may reduce energy demands in comparison with plasma alone. Blanquet *et al* [54] used a small pyrolytic reactor and tars made from wood pellets and studied their decomposition by plasma catalytic steam reforming in DBD with Ni/Al<sub>2</sub>O<sub>3</sub> catalyst at 250 °C. The results showed that the combination of plasma with catalyst produced less liquid, more gaseous by-products and the lowest coke deposition level on the catalyst surface compared to systems of either catalyst or plasma alone.

The objective of this work was to investigate tar removal (conversion) by NTP generated by atmospheric pressure DBD either alone or in combination with various packing materials, including catalysts (TiO<sub>2</sub>, Pt/ $\gamma$ -Al<sub>2</sub>O<sub>3</sub>) and other dielectric

materials ( $\gamma$ -Al<sub>2</sub>O<sub>3</sub>, glass beads). The packing materials were chosen for various reasons. The glass beads were selected as a dielectric material without any specific catalytic activity, while  $\gamma$ -Al<sub>2</sub>O<sub>3</sub> was selected as the most common bulk material for the supported catalysts. The Pt/ $\gamma$ -Al<sub>2</sub>O<sub>3</sub> catalyst was selected as being amongst the best catalysts reported for naphthalene oxidation. Finally, TiO<sub>2</sub> was selected as the most common photocatalyst that can be activated by either UV radiation emitted by NTP [55, 56] or the highly energetic electrons of NTP [21, 57, 58], and also because it is considered to be one of the most efficient photocatalysts for VOC treatment [59, 60]. Naphthalene was chosen as a model tar compound because it is the simplest PAH and one of the most difficult tar compounds to decompose or reform [61]. The effects of the discharge operating parameters (the amplitude and frequency of the applied voltage, the discharge power), carrier gas and packing material on naphthalene removal and the formation of gaseous and solid by-products were investigated. To achieve highly efficient thermal decomposition of tars, temperatures above 950 °C–1100 °C are usually required, while slightly lower temperatures are needed for catalytic methods [62, 63]. When plasma or plasma catalytic methods are employed for tar removal the operating temperature can be decreased further to several hundred degrees [3, 44, 47, 52, 53]. In contrast to the existing works on naphthalene removal, we performed our experiments at a relatively low operating temperature (below 150 °C). Even though the temperature was low, it was sufficient to activate the catalyst via contact with the NTP and to obtain reasonable removal and energy efficiency.

## 2. Experimental setup and methods

The experimental setup is depicted in figure 1. NTP was generated by DBD reactors of cylindrical geometry operating in the streamer discharge mode. The reactors consisted of a quartz glass tube with an inner diameter of 1.5 cm and a length of 10 cm. A tungsten wire with a diameter of 0.2 mm placed in the axis of the tube was used as a high voltage electrode, while an aluminium foil sheet wrapped around the outer surface of the quartz tube served as a ground electrode. The plasma catalytic reactors were packed with various materials, either glass beads or dielectric/catalytic pellets ( $\gamma$ -Al<sub>2</sub>O<sub>3</sub>, Pt/ $\gamma$ -Al<sub>2</sub>O<sub>3</sub> and TiO<sub>2</sub>) with diameter of 2–3 mm. The reactors were powered by an AC high voltage power supply consisting of a function generator (GwInstek SFG-1013), signal amplifier (Omnitronic PAP-350) and high voltage transformer. The power supply system allowed us to vary the amplitude and frequency of the applied voltage. The waveform of the applied voltage was measured by a high voltage probe (Tektronix P6015A) and the discharge current pulses were measured by a current probe (Pearson Electronics 2877) connected to a digital oscilloscope (Tektronix TDS2024). The power consumption of the reactor was evaluated using the Lissajous figure method with an 82 nF capacitor and a voltage probe (Tektronix P2220).

Ambient air, oxygen or nitrogen were used as the carrier gases and their gas flow rate was controlled by flow meters.

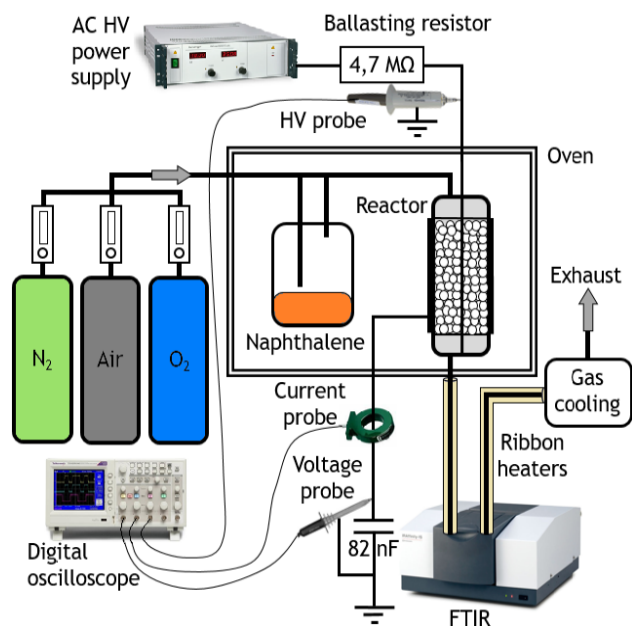


Figure 1. Experimental setup.

The carrier gases were enriched with naphthalene vapours and then led to the plasma reactor. Naphthalene (CentralChem) was used as a model tar compound due to its stability and the difficulty of decomposing it. It is a white solid crystalline compound with low saturated vapour pressure at ambient temperature ( $\sim 13$  Pa at  $25^\circ\text{C}$ ) and decent saturated vapour pressure at  $100^\circ\text{C}$  ( $\sim 2.6$  kPa). The experimental system, including the plasma reactor and gas lines, was heated using an electric oven and ribbon heaters to a temperature of  $100^\circ\text{C}$ . With plasma discharge, the temperature inside the reactor gradually increased up to a maximum of  $121^\circ\text{C}$ . The initial concentration of naphthalene in the carrier gas was approximately 0.5 vol.% and the total gas flow was set to  $0.5\text{ l min}^{-1}$ . The gaseous and solid by-products of naphthalene decomposition were analysed by means of FTIR spectrometry (Shimadzu IR-Affinity 1S).

The performance of the plasma and the plasma catalytic reactors was evaluated with the help of the following variables: specific input energy (i.e. energy density per volume) (SIE), naphthalene removal efficiency (NRE) and energy efficiency (EE). They were calculated according to equations (1)–(3).

- Specific input energy (SIE):

$$\text{SIE}(\text{J/L}) = \frac{P}{Q}, \quad (1)$$

where  $P$  and  $Q$  represent the input power and total gas flow rate, respectively.

- Naphthalene removal efficiency (NRE)  $\eta$ :

$$\eta (\%) = \left(1 - \frac{[\text{naph}]}{[\text{naph}]_0}\right) * 100, \quad (2)$$

where  $[\text{naph}]$  and  $[\text{naph}]_0$  represent the input and output concentrations of naphthalene, respectively.

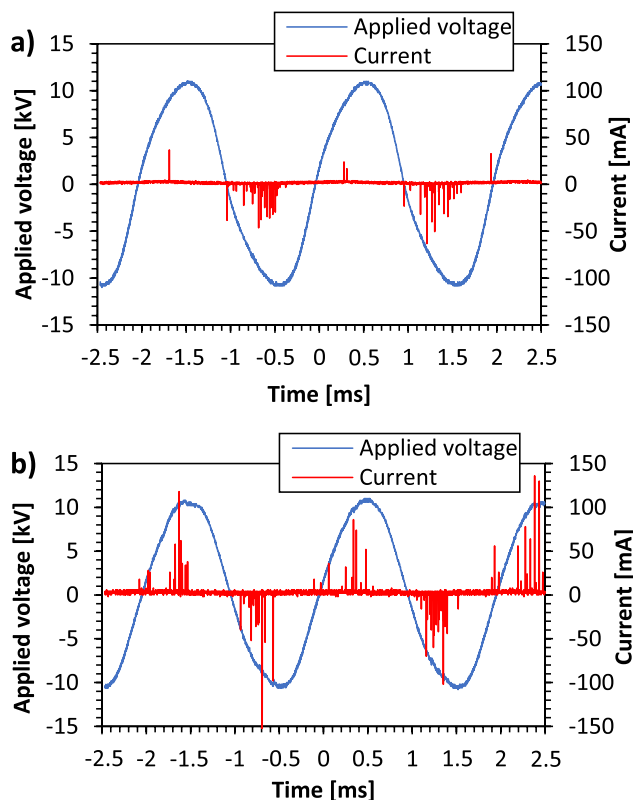


Figure 2. Voltage and current waveforms of plasma reactors: (a) without catalyst and (b) with  $\text{TiO}_2$  catalyst (ambient air, 11 kV, 500 Hz).

- Energy efficiency (EE):

$$\text{EE} (\text{g kWh}^{-1}) = \frac{\eta[\text{naph}]_0}{\text{SIE}}. \quad (3)$$

Some additional parameters are important to evaluate the quality of the naphthalene removal process: concentration, selectivity and yield of the gaseous and solid by-products, and total carbon balance. Although the analysis of gas and solid by-products showed the presence of various carbon-containing products in the spectra, only the concentrations of CO and  $\text{CO}_2$  were measured absolutely. All other gaseous and solid by-products were only detected qualitatively and a few products were only identified via their functional groups. To calculate the selectivity or the total carbon balance properly, the absolute concentrations of the products must be known, as calculations based solely on the concentrations of CO and  $\text{CO}_2$  can underestimate the real values achieved in the experiments. Therefore, in this work, the carbon balance is not shown, and only the concentrations of the two major gaseous products CO and  $\text{CO}_2$  are presented.

### 3. Results and discussion

#### 3.1. Discharge power consumption and chemical activity

Figure 2 presents typical voltage and current waveforms of the plasma reactor without and with  $\text{TiO}_2$  catalyst. In the plasma reactor (figure 2(a)), the discharge current pulses occurred

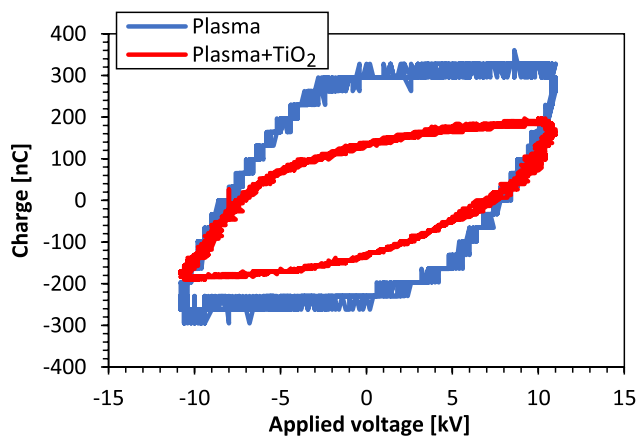


**Figure 3.** Lissajous figures for the plasma reactors without and with TiO<sub>2</sub> catalyst (ambient air, 11 kV, 500 Hz).

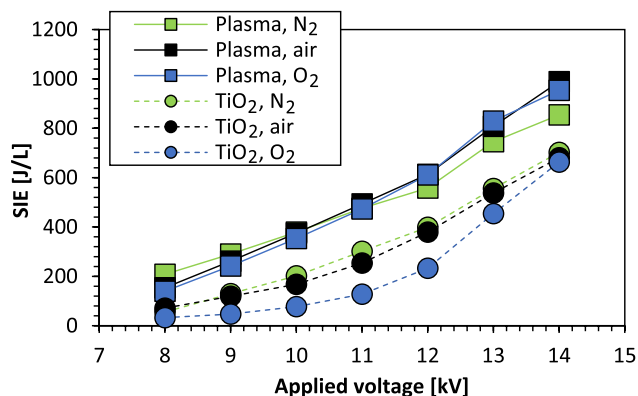


**Figure 4.** SIE as a function of the amplitude of the applied voltage for plasma and plasma catalytic TiO<sub>2</sub> reactors and various carrier gases (500 Hz).

predominantly in the negative half-period of the applied voltage, while in the plasma catalytic reactor (figure 2(b)), the pulses occurred in both the negative and positive half-periods. At the given voltage, the amplitudes of the current pulses were usually higher in the plasma catalytic reactor compared to the plasma reactor. For all plasma catalytic reactors, the discharge onset/ignition voltage was found to be lower (approximately 2–3 kV) compared to the plasma reactor (approximately 6 kV). The ignition voltage corresponded to the amplitude of the applied voltage at the moment when the first discharge current pulses were observed on the oscilloscope. The lower ignition voltage with the plasma catalytic reactor is due to the presence of packing material that usually enhances local electric field strengths and reduces the discharge ignition voltage [64].

Lissajous figures were recorded to evaluate the power consumption of the reactors and consequently the specific input energy SIE. Figure 3 shows typical Lissajous figures for the plasma reactor without and with TiO<sub>2</sub> catalyst. Further, figures 4 and 5 show the specific input energy SIE of the plasma and the plasma catalytic reactors as a function of amplitude of the applied voltage. The SIE value increased with the amplitude of the applied voltage (from 8 to 14 kV) and the frequency (from 200 Hz to 500 Hz). As figure 4 shows, in the plasma reactor the carrier gas (ambient air, nitrogen, oxygen) only had a small effect on the SIE. In the plasma catalytic

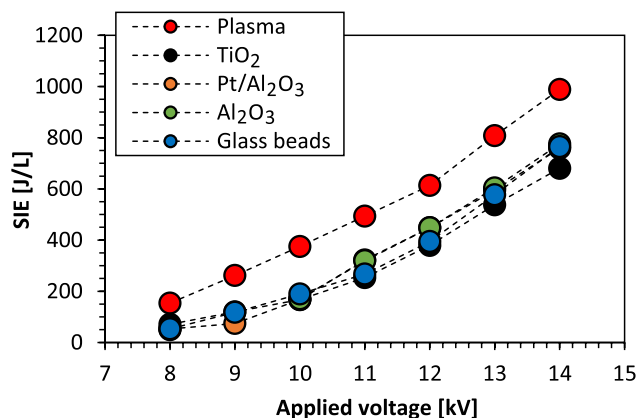


**Figure 5.** SIE as a function of the amplitude of the applied voltage for plasma and plasma catalytic reactors (ambient air, 500 Hz).

TiO<sub>2</sub> reactor, the SIE was similar in ambient air and nitrogen, while the SIE was slightly lower in oxygen. The effect of packing material on the SIE was found to be negligible as the SIE was almost the same for all of the plasma catalytic reactors with different packings. On the other hand, at the given applied voltage, the SIE of the plasma reactor was higher than the SIE of the plasma catalytic reactors (figure 5). The presence of the packing material in the plasma reactor decreases the discharge power under the same operating conditions. This effect can be explained by a higher space charge effect in plasma catalytic reactors, which reduces the discharge current and corresponding output power [25]. Although the amplitudes of the current pulses in plasma catalytic reactors were usually higher (figure 2), estimating the power consumption while only considering the amplitudes of the current pulses is usually insufficient as the number of pulses (pulse repetition rate) should also be considered.

Prior to the tests with naphthalene, the chemical activity of the plasma and plasma catalytic reactors used was evaluated in all carrier gases (ambient air, nitrogen, oxygen) without naphthalene by monitoring concentrations of various gaseous species formed in the plasma (e.g. O<sub>3</sub>, NO<sub>x</sub>) by means of FTIR spectrometry. This was done to determine what kind of neutral molecular species plasma can generate that could possibly take part in the naphthalene decomposition process once naphthalene is present in the gas mixture. In oxygen, ozone (O<sub>3</sub>) was the only gaseous product found in the spectra with concentrations of approximately 1500 and 1300 ppm (at 11 kV, 500 Hz) for plasma and the plasma catalytic TiO<sub>2</sub> reactor, respectively. In ambient air, the concentration of O<sub>3</sub> was indeed smaller. In plasma and plasma catalytic Pt/ $\gamma$ -Al<sub>2</sub>O<sub>3</sub> and TiO<sub>2</sub> reactors, it only reached approximately 180 ppm, 160 ppm and 210 ppm (at 11 kV, 500 Hz), respectively. The highest O<sub>3</sub> concentration was found for the reactor with  $\gamma$ -Al<sub>2</sub>O<sub>3</sub> packing (approximately 330 ppm) at the same operating conditions. In addition to O<sub>3</sub>, and depending on the discharge power, small amounts of various nitrogen compounds were also observed in ambient air spectra, mainly nitrous oxide N<sub>2</sub>O (up to 55 ppm) and nitric acid (HNO<sub>3</sub>). On the other hand, nitric oxide (NO) was not observed at all and nitrogen dioxide (NO<sub>2</sub>) (approximately 250 ppm) was only detected in the plasma reactor packed with

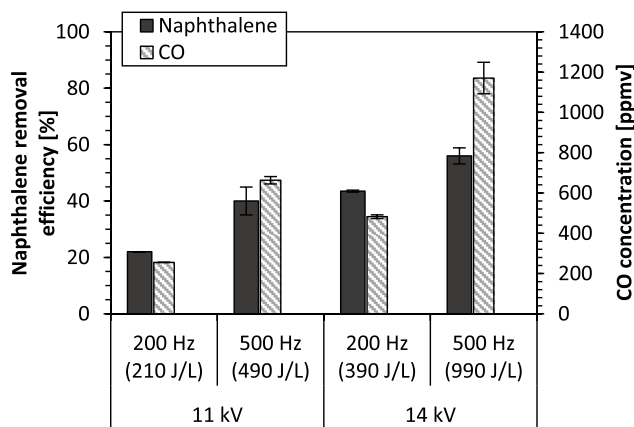


**Figure 6.** NRE and CO concentration for the *plasma reactor* as a function of the amplitude and frequency of the applied voltage (ambient air).

glass beads at the highest SIE (approximately  $700 \text{ J l}^{-1}$ ). In nitrogen carrier gas, no specific gaseous compounds were found in the FTIR spectra.

### 3.2. The effect of applied voltage and discharge power

Figures 6 and 7 show the naphthalene removal efficiency (NRE) in plasma (figure 6) and plasma-catalytic  $\text{TiO}_2$  (figure 7) reactors as a function of the amplitude and frequency of the applied voltage. The corresponding SIE values are also given. In both reactors, the NRE increased with the increase of the amplitude and frequency of the applied voltage and it was always significantly higher in the plasma catalytic reactors compared to the plasma reactor. Moreover, in the plasma catalytic reactors, higher NRE was achieved with lower energy consumption, i.e. at lower SIE. As the figures show, for the given applied voltage and frequency (14 kV, 500 Hz), the NRE of the plasma catalytic  $\text{TiO}_2$  reactor was 95% ( $680 \text{ J l}^{-1}$ ), while the NRE of the plasma reactor was only 56% ( $990 \text{ J l}^{-1}$ ). This result demonstrates the positive role of  $\text{TiO}_2$  catalyst in the naphthalene removal process, as it enhances the NRE and reduces energy demands in comparison with plasma processing alone.

Various by-products of the naphthalene decomposition were detected by FTIR in the gas phase and also as solid deposits found in the reactor and in the FTIR gas cell. The concentration of the by-products depended on the carrier gas, the reactor packing material and the discharge power. The main gaseous products of naphthalene decomposition identified in the FTIR spectra were CO,  $\text{CO}_2$ ,  $\text{H}_2\text{O}$  and  $\text{HCOOH}$ , along with the  $\text{N}_2\text{O}$  and  $\text{O}_3$  formed by the reactions in the carrier gas. In nitrogen, no gaseous products were found, while in ambient air and oxygen, CO and  $\text{CO}_2$  dominated. As the net  $\text{CO}_2$  concentration analysed by FTIR was often affected by the variation of the background  $\text{CO}_2$  in the laboratory, while the CO concentration was not, the latter is given here as an indicator of naphthalene removal. The CO concentration in the plasma and plasma catalytic  $\text{TiO}_2$  reactors as a function of the amplitude and frequency of the applied voltage is presented in figures 6 and 7, next to the NRE data points. Similar

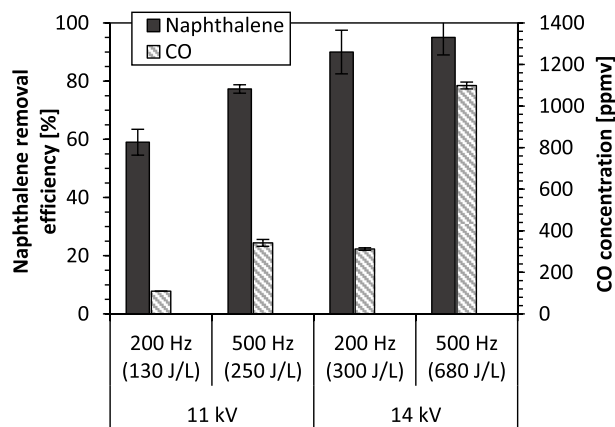


**Figure 7.** NRE and CO concentration for the *plasma catalytic  $\text{TiO}_2$  reactor* as a function of the amplitude and frequency of the applied voltage (ambient air).

to the NRE, the CO concentration increased with the increase of the amplitude and frequency of the applied voltage, as well as the discharge power, i.e. SIE. As the figures show, the CO concentration varied between 100–1200 ppm depending on the discharge power and reactor type. In the same experiments, the corresponding concentration of  $\text{CO}_2$  was between 100–1500 ppm. Although the CO and  $\text{CO}_2$  concentrations increased with the SIE, their production depended on the reactor type being used.

In addition to the by-products detected in the gas phase, solid by-products and deposits were found on the reactor walls and packing material, as well as in the FTIR gas cell. More details on these results are presented and discussed in the following sections.

### 3.3. The effect of carrier gas

The carrier gas may have a significant effect on the chemical process of naphthalene decomposition, its efficiency and by-products, as different reactive species may be formed. With nitrogen as a carrier gas, the active species formed by the plasma originate from nitrogen, such as  $\text{N}_2(\text{A})$  or  $\text{N}$  [37, 39, 41, 65]. If oxygen is present, atomic oxygen radicals ( $\text{O}^3\text{P}$ ,  $\text{O}^1\text{D}$ ) and ozone ( $\text{O}_3$ ) are successfully generated [37, 39, 41]. In ambient air, excited nitrogen molecules ( $\text{N}_2(\text{A,B,C})$ ) can dissociate oxygen molecules, resulting in the formation of O radicals [66, 67], and residual humidity may cause the formation of OH radicals through the dissociation of  $\text{H}_2\text{O}$  molecules. All these highly reactive species, along with several others (e.g.  $\text{NH}$ ,  $\text{CH}$ ) generated by collisions between energetic electrons and carrier gas molecules in the plasma, can oxidise or reduce naphthalene molecules effectively.

Figure 8(a) shows the effect of carrier gases on the NRE in both the plasma and plasma catalytic reactors. In nitrogen carrier gas, the NRE was generally very poor (below 25%) in both reactors. The absence of oxygen in the carrier gas led to the oxidation reactions being entirely restrained and no CO or  $\text{CO}_2$  was detected in the spectra. The removal of naphthalene was most probably governed by the species such as  $\text{N}_2(\text{A})$  or  $\text{N}$  [37, 39, 41, 65]. The effect of  $\text{N}_2(\text{A})$  on naphthalene

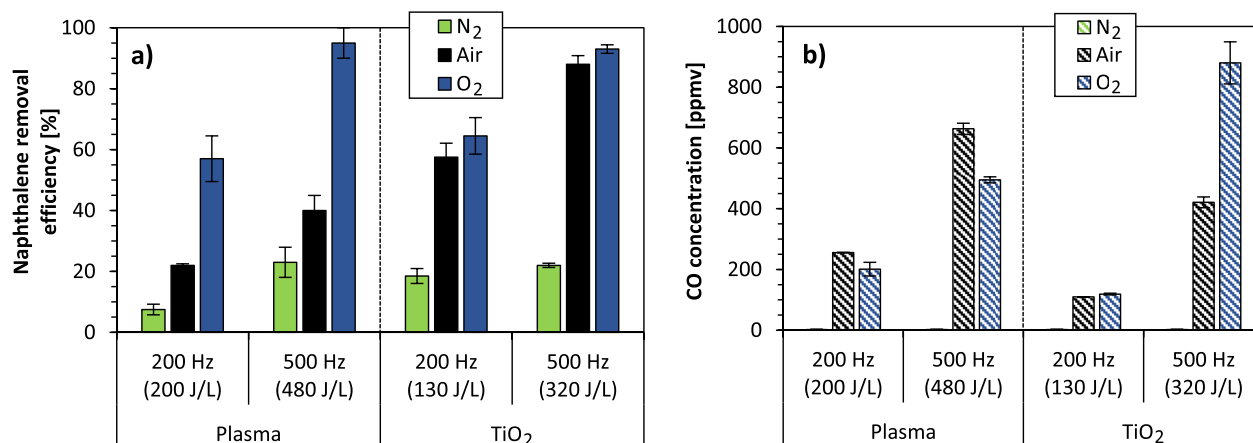


**Figure 8.** (a) NRE and (b) CO concentration in plasma and plasma catalytic TiO<sub>2</sub> reactors in various carrier gases.

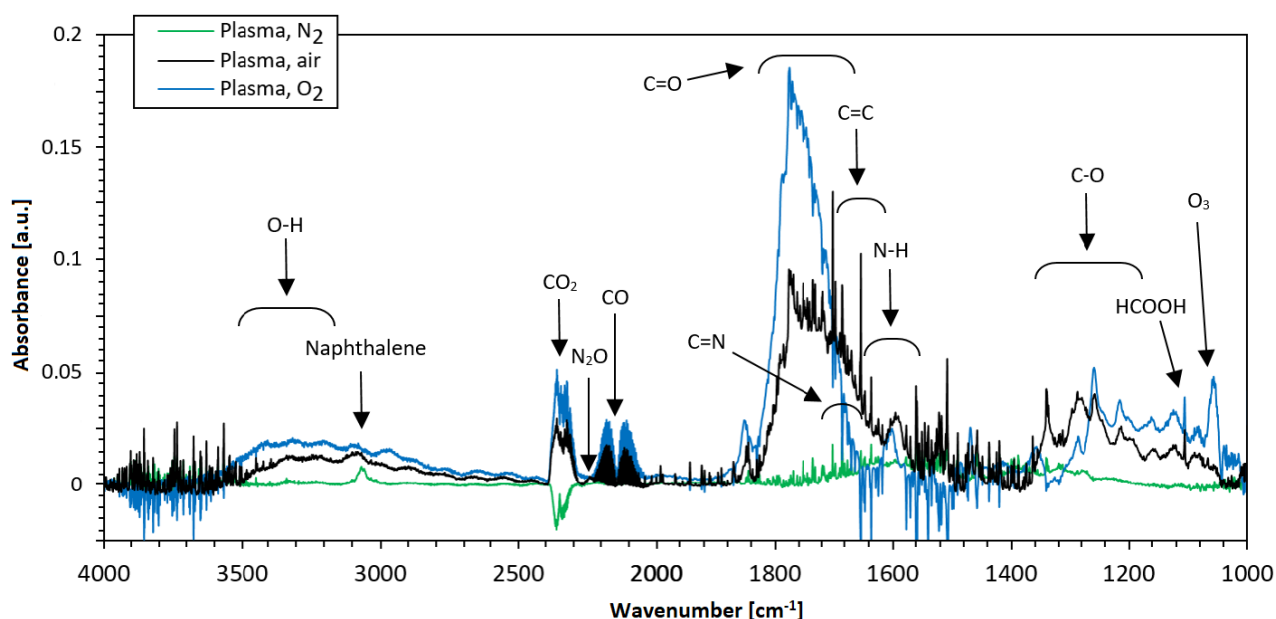


**Figure 9.** Infrared absorption spectra of gaseous and solid by-products of naphthalene decomposition for the plasma reactor and different carrier gases.

removal is probably dominant in comparison with other the molecular species formed by the discharge, such as N<sub>2</sub>(C) and N<sub>2</sub>(B), as these quickly deexcite to N<sub>2</sub>(A) when formed. The production of atomic nitrogen species in discharges such as DBD or streamer corona is usually small and their effect on naphthalene removal is probably weak. Through collisions with the naphthalene molecules they may initiate reactions that lead to its removal via the dissociation of C–H and C–C chemical bonds. According to Wu *et al* [39], the final products of naphthalene decomposition in nitrogen are usually various mono- and hetero- nitrogen-containing aromatic compounds. In nitrogen carrier gas, especially without catalytic packing material, aerosol particles can be formed during naphthalene decomposition. Their concentration decreases gradually with increasing oxygen as more reactive oxygen species are generated and lead to the oxidation of naphthalene and particles to CO and CO<sub>2</sub> [39].

In ambient air, the naphthalene decomposition increased rapidly and the NRE was significantly higher than that in

nitrogen. The NRE in the plasma reactor reached approximately 22% and 40% for 200 and 480 J l<sup>-1</sup>, respectively. In the plasma catalytic reactor with TiO<sub>2</sub> the NRE was even higher and reached approximately 58% and 88% for 130 and 320 J l<sup>-1</sup>, respectively. This was accompanied by the formation of CO and CO<sub>2</sub> (up to 450 ppm and 470 ppm, respectively) (TiO<sub>2</sub>, 320 J l<sup>-1</sup>). Along with the formation of COx and H<sub>2</sub>O, a limited amount of nitrous oxide N<sub>2</sub>O and formic acid HCOOH was also detected (figure 9). The increase of the NRE and gaseous by-products is mainly due to the formation of atomic oxygen radicals (O(<sup>3</sup>P), O(<sup>1</sup>D))) and ozone (O<sub>3</sub>). The O atoms can react directly with naphthalene and produce oxygen-containing hydrocarbons or hydrocarbons with fewer carbon atoms. Their further oxidation may lead to aromatic ring opening, the formation of aliphatic hydrocarbons and the production of CO and CO<sub>2</sub> [39]. Compared to nitrogen carrier gas, the quantity of nitrogen-containing compounds in ambient air was reported to be significantly reduced.

When oxygen was the carrier gas, the NRE reached almost 100% in both the plasma and plasma catalytic reactors. These results confirmed the dominant role of oxygen radicals and ozone, as was also reported in [3, 39]. The concentration of CO, CO<sub>2</sub> and H<sub>2</sub>O as the final stable gaseous by-products of the naphthalene decomposition increased significantly compared with that for the ambient air experiments. Wu *et al* suggested [39] that naphthalene decomposition is first initiated by dehydrogenation and oxidation, followed by deep oxidation to CO and CO<sub>2</sub>. Oxygen plays an important role in CO and CO<sub>2</sub> production. In the plasma reactor in oxygen, as compared to ambient air, a smaller CO concentration (figure 8(b)) and a correspondingly higher CO<sub>2</sub> concentration (up to 400 ppm) was detected. This was the result of improved oxidation governed by O radicals and ozone (O<sub>3</sub>). Ozone is formed through the electron impact dissociation of O<sub>2</sub> and recombination with O atom. Its concentration reflects the generation of O radicals in the discharge and increases gradually with O<sub>2</sub> concentration. We found 1500 ppm of O<sub>3</sub> in oxygen carrier gas without naphthalene (11 kV, 500 Hz), compared to only ~850 ppm with naphthalene. Therefore, it is possible to assume that the ozone was used effectively for the oxidation of naphthalene. In the plasma catalytic TiO<sub>2</sub> reactor, both the CO and CO<sub>2</sub> concentration increased if oxygen replaced ambient air as the carrier gas. The CO concentration achieved the maximal value of approximately 900 ppm (figure 8(b)), while the CO<sub>2</sub> concentration was much higher, with values of up to approximately 1900 ppm.

In all of the reactors and tested conditions, we obtained the lowest NRE in nitrogen carrier gas and a significantly higher NRE in air/oxygen carrier gases. However, it is also possible to achieve a higher NRE in nitrogen compared to oxygen-containing mixtures, as reported by Abdelaziz *et al* [41]. They found that the naphthalene removal efficiency in oxygen/air and nitrogen depends strongly on energy density and better efficiency can only be achieved in nitrogen at very low energy density (below 1 J l<sup>-1</sup>).

Figure 9 shows the FTIR spectra of gaseous and solid by-products of naphthalene decomposition in the plasma reactor without packing material for different carrier gases. The main absorption bands correspond to basic gaseous compounds, including CO, CO<sub>2</sub>, N<sub>2</sub>O, O<sub>3</sub> and HCOOH. However, there are several other absorption bands that belong to organic functional groups (such as C=O, C=C, C-O, C=N, N-H or O-H). The presence of these functional groups indicates the production of various hydrocarbons, formed as a result of naphthalene decomposition either in the gas phase or as solid by-products. These solid by-products were analysed using two different techniques. During the experiments, the deposits that formed on the IR gas cell windows were analysed directly using a transmission FTIR technique. These results are shown in figure 9. After the experiments, the deposits found on reactor walls were collected and analysed using the KBr pellet method. The FTIR spectra of the solid by-products collected from the reactor walls and those deposited on the IR gas cell windows were compared and found to be very similar.

The identification of the exact by-products of naphthalene decomposition by using FTIR spectroscopy, especially those

in the solid phase, is not trivial. In the case of complex molecules, often only their functional groups can be determined and identified. The available literature on naphthalene removal chemistry and FTIR spectra libraries was reviewed against our spectra to identify possible by-products [3, 39, 52, 53, 62, 65, 68, 69]. Among the by-products of naphthalene decomposition, various compounds have been reported, namely—1,4-naphthoquinone, phthalic anhydride, phthalaldehyde, phthalide, phthalic acid, maleic anhydride, 1,4-benzoquinone, naphthol, phenylethyne, naphthalene dione, dimethyl phthalate, trimethyl benzenes, benzaldehyde, benzonitrile, benzene, toluene, xylenes, acetophenone benzoic acid, benzyl alcohol and a few other nitrogen- and oxygen-containing polyaromatic compounds, as well as aliphatic compounds resulting from the aromatic ring opening reactions. The detailed analysis of our spectra allowed us to identify 1,4-naphthoquinone and phthalic anhydride among the products, and, with a lower quality of match, maleic anhydride, 1,4-benzoquinone and phthalaldehyde. As the analysis of the solid by-products was only performed qualitatively, and not quantitatively, and some of the by-products have not been identified completely (only some of their functional groups), we cannot offer a clear conclusion about the total toxicity of products. A detailed analysis of the solid by-products of naphthalene decomposition is yet to be performed and will be part of future work after the installation of appropriate diagnostics. On the other hand, our analysis excluded compounds such as naphthol, benzaldehyde, acetophenone, benzoic acid, phenylethyne or phenyl-naphthalene as potential by-products of naphthalene decomposition. The compounds found in our spectra represent organic gaseous and solid intermediates of naphthalene decomposition and indicate its incomplete oxidation to the desired products of CO<sub>2</sub> and H<sub>2</sub>O.

### 3.4. The effect of packing material

The effects of packing materials on naphthalene removal and the formation of gaseous and solid by-products were investigated, along with the effects of discharge properties (section 3.2) and carrier gas (section 3.3). In the past, various materials and catalysts have been tested for naphthalene removal, e.g. TiO<sub>2</sub> [70–73], Pt/Al<sub>2</sub>O<sub>3</sub>, V-modified Pt/Al<sub>2</sub>O<sub>3</sub> or Pt/SiO<sub>2</sub> [74–77], H<sub>2</sub>-mordierite [78], Ni-dolomite [79] or CeO<sub>2</sub> catalyst [69], both in standalone catalytic systems and in combination with NTP, with various NRE and by-products. In this section, we present our results obtained using four different packing materials with very distinct or no catalytic properties (TiO<sub>2</sub>, Pt/γ-Al<sub>2</sub>O<sub>3</sub>, γ-Al<sub>2</sub>O<sub>3</sub>, glass beads).

Figure 10 show the NRE and corresponding CO and CO<sub>2</sub> concentrations obtained when using various packing materials for an SIE of 150 and 320 J l<sup>-1</sup> at 200 and 500 Hz in ambient air, respectively. It is clearly seen that, at the given SIE, the smallest NRE was obtained with plasma reactor, while reactors with packing material showed higher NRE, as well as higher EE. Corresponding higher CO and CO<sub>2</sub> concentrations were found in the plasma catalytic TiO<sub>2</sub> and Pt/γ-Al<sub>2</sub>O<sub>3</sub> reactors (figure 10(b)).

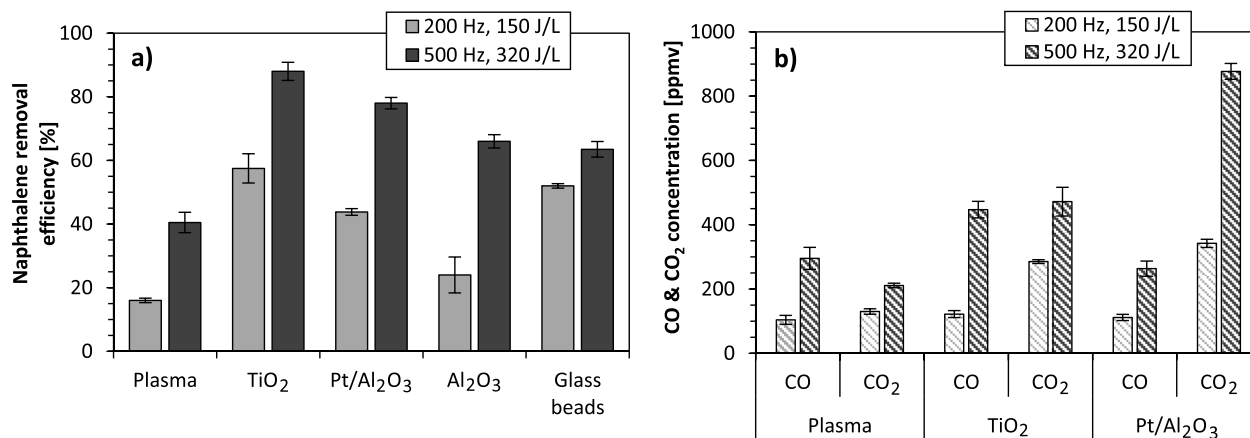


**Figure 10.** (a) NRE and (b) CO and CO<sub>2</sub> concentration when using different reactors without/with various packing materials (ambient air).

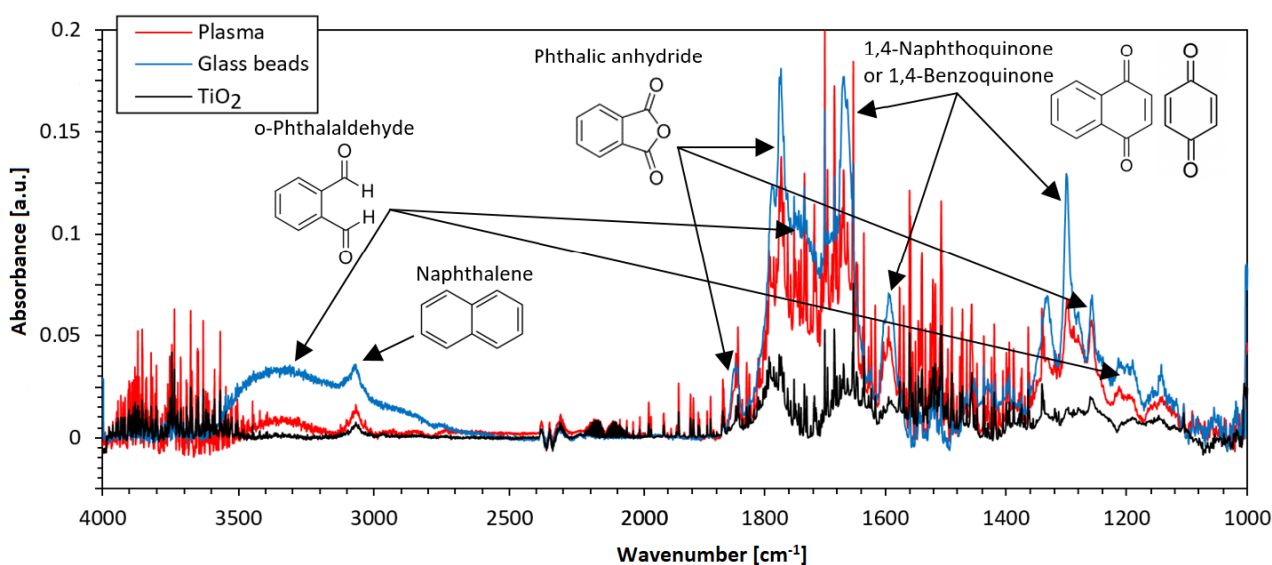


**Figure 11.** Infrared absorption spectra of gaseous and solid by-products of naphthalene decomposition for a plasma reactor and plasma catalytic reactors with TiO<sub>2</sub> catalyst and glass bead packing (ambient air).

The highest NRE of approximately 58% and 88% for 150 and 320 J l<sup>-1</sup>, respectively, were reached in the plasma catalytic reactor with metal oxide TiO<sub>2</sub> catalyst (figure 10(a)). TiO<sub>2</sub> is one of the most commonly used photocatalysts and usually shows superb oxidation performance. When used in a plasma catalytic reactor, the photocatalyst can be activated by the UV radiation emitted by the plasma [55, 56], or it can be activated directly by highly energetic electrons [21, 57, 58]. In contrast to the plasma reactor or the reactors with other packing materials, the lowest relative concentration of solid by-products in the FTIR spectra was observed with the TiO<sub>2</sub> catalyst (figure 11). Not only was the highest NRE obtained with the TiO<sub>2</sub> catalyst, but the highest EE was also obtained (approximately 289 and 207 g kWh<sup>-1</sup> for 150 and 320 J l<sup>-1</sup>, respectively). It is interesting to note that a higher EE of 289 g kWh<sup>-1</sup> was obtained for a lower SIE of 150 J l<sup>-1</sup> to

320 J l<sup>-1</sup>, the NRE only increased by a factor of 1.5 (from 58% to 88%).

Various studies on catalytic oxidation of aromatic hydrocarbons have shown that metal-supported catalysts can often be as effective as metal oxide catalysts. Among the metal-supported catalysts used for hydrocarbon oxidation, Pt has been identified as being more active than Pd and Ru, and Pt supported on  $\gamma$ -Al<sub>2</sub>O<sub>3</sub> is the most active catalyst [74]. Therefore, along with the metal oxide TiO<sub>2</sub> catalyst, metal-supported Pt/ $\gamma$ -Al<sub>2</sub>O<sub>3</sub> was also tested. In our tests, the Pt/ $\gamma$ -Al<sub>2</sub>O<sub>3</sub> catalyst showed a slightly lower NRE than TiO<sub>2</sub>, namely 78% and 88% for 320 J l<sup>-1</sup>, respectively (figure 10(a)). Smaller NRE probably occurred because the Pt/ $\gamma$ -Al<sub>2</sub>O<sub>3</sub> catalyst needs an operating temperature that is higher than the 121 °C used in our study. Shie *et al* [75] reported that efficient oxidation of naphthalene with Pt/ $\gamma$ -Al<sub>2</sub>O<sub>3</sub> catalyst without plasma can be observed at a temperature of 150 °C, i.e. higher than in our system. Moreover, Sellick *et al* found that catalysts were inactive below 150 °C, only showing some trace conversion to

CO<sub>2</sub> above 150 °C [76]. However, temperature is not the only parameter determining Pt/ $\gamma$ -Al<sub>2</sub>O<sub>3</sub> activity. It also depends on average platinum particle size, their dispersion on the support (number of active sites) and the material of the support [76, 80, 81]. In our experiments, we only used one type of Pt/ $\gamma$ -Al<sub>2</sub>O<sub>3</sub> catalyst, and therefore we were unable to evaluate the effect of these physical properties on catalyst activity. The NRE can be also affected by the presence of ozone and its destruction over the catalyst. Pt/ $\gamma$ -Al<sub>2</sub>O<sub>3</sub> is known for its ability to lower the temperature for ozone decomposition. The decomposition of ozone is a thermodynamically favoured reaction. Without the catalyst, the ozone can be thermally decomposed efficiently at temperatures from approximately 115 °C to 200 °C, when its half-life is relatively short. However, the temperature can be reduced down to room temperature when Pt/ $\gamma$ -Al<sub>2</sub>O<sub>3</sub> catalyst is used. Such catalytic oxidation of naphthalene in the presence of O<sub>3</sub> not only decreases the reaction temperature, but also increases the mineralization of naphthalene [77]. Although the NRE with the Pt/ $\gamma$ -Al<sub>2</sub>O<sub>3</sub> catalyst was only slightly lower than that with the TiO<sub>2</sub> catalyst, the corresponding CO concentration was significantly smaller and the CO<sub>2</sub> concentration was significantly higher with the Pt/ $\gamma$ -Al<sub>2</sub>O<sub>3</sub> catalyst (figure 10(b)). This result implies improved oxidation when compared to other packing materials or plasma alone. Not only was the NRE lower with the Pt/ $\gamma$ -Al<sub>2</sub>O<sub>3</sub> catalyst compared to the TiO<sub>2</sub> catalyst, but the EE was also lower (approximately 220 and 184 g kWh<sup>-1</sup> for 150 and 320 J l<sup>-1</sup>).

Finally, the effect of  $\gamma$ -Al<sub>2</sub>O<sub>3</sub> pellets and glass beads as packing material was studied. The NRE and the EE for  $\gamma$ -Al<sub>2</sub>O<sub>3</sub> pellets showed similar results to those for glass beads for 320 J l<sup>-1</sup> (the NRE was 66 and 64%, while the EE was 155 and 150 g kWh<sup>-1</sup>, respectively). It is worth mentioning that for a lower SIE of 150 J l<sup>-1</sup>, the situation is different. The reactor with  $\gamma$ -Al<sub>2</sub>O<sub>3</sub> pellets showed an NRE of 24% and an EE of 121 g kWh<sup>-1</sup>, while the reactor with glass beads showed an NRE of 52% and an EE of 261 g kWh<sup>-1</sup>. Although glass beads and  $\gamma$ -Al<sub>2</sub>O<sub>3</sub> are materials without specific catalytic properties, the plasma reactors packed with them reached a higher NRE than plasma reactors without them at the same SIE. This can principally be explained by enhanced discharge volume distribution. Kim *et al* [80] studied the effect of packing material on discharge and plasma quality and distribution. They found that the material conductivity affects the formation of surface streamers, determines the surface area covered by plasma and has a strong influence on catalyst activity. Butterworth *et al* [64] tested materials with various dielectric constants and found two different modes of discharge, depending on the applied voltage and dielectric constant. For low dielectric constant materials and with high applied voltage, discharge mainly occurred in the surface streamer mode. However, discharge quality is also related to other properties of the materials, such as their conductivity and porosity. Ray *et al* [82] reported that glass bead packing improved the discharge strength, decreased the ignition voltage and increased the transferred charge compared to reactors without packing. The interaction of glass beads with plasma improved the performance of the plasma and its chemical activity and resulted in

higher removal efficiency when compared to plasma reactors, as we also observed in our experiments.

Figure 11 shows the FTIR spectra of the gaseous and solid products formed as a result of naphthalene decomposition. A comparison of plasma reactors and reactors packed with glass beads and TiO<sub>2</sub> catalyst is presented. In addition to the main gaseous products (CO, CO<sub>2</sub>, H<sub>2</sub>O, HCOOH), we positively identified 1,4-naphthoquinone and phthalic anhydride in the spectra. In contrast to the spectra for the plasma reactor and the glass bead packing, a lower concentration of solid by-products was observed in the plasma catalytic TiO<sub>2</sub> reactor. This is evidence that more effective oxidation of naphthalene to desired gaseous by-products can be achieved with a plasma catalytic system in comparison with a plasma system. Moreover, the decomposition of hydrocarbons, especially VOCs, with plasma alone is generally recognised for lower CO<sub>x</sub> production, higher production of by-products and excessive formation of undesirable organic aerosols as a result of incomplete oxidation [83]. When a packing material with large surface area is used with the plasma, the efficiency evaluation and product analysis for naphthalene removal must be performed very carefully. The reason for this is the fact that naphthalene can be readily adsorbed onto the surface of the catalyst, potentially leading to overestimation of its oxidation activity and the NRE, especially at lower temperatures. The evaluation of the NRE may also lead to erroneous conclusions due to the possible formation of by-products [76]. Hence, the production of CO and CO<sub>2</sub> and not the NRE must be considered when evaluating the oxidation activity of the catalyst. To avoid overestimation in our results we performed long-lasting 1 d experiments (for different applied voltages and frequencies) to be sure that the concentrations of naphthalene and by-products recognized in the spectra stabilized or saturated. The experiments were repeated several times using either the same (old) packing material, or a fresh material. If the old packing material was used and the experiments were repeated, we observed a drop in the NRE (approximately 6% per experiment).

The results and corresponding discussion on the effects of discharge power, carrier gas and packing materials on naphthalene removal and the formation of by-products are finally supplemented by the comparison of our results with the results from other studies. As mentioned earlier in this paper, tar removal by plasma and plasma catalysis have been studied by several research groups in recent years. In most of these studies, toluene was chosen as a target tar compound. However, toluene is a monoaromatic tar compound, and is less thermally stable and much easier to decompose than polyaromatic naphthalene [62]. Therefore, the results for the removal of toluene and naphthalene by plasma and plasma catalytic means cannot be directly compared with respect to the NRE and EE. Table 1 only summarizes the results for naphthalene removal by means of plasma and plasma catalysis. Various discharge types, catalysts, temperatures, carrier gases, gas mixtures and initial naphthalene concentrations have been used, and so only a rough comparison of results is possible. For instance, Gao *et al* [52] used positive corona discharge with MnO<sub>2</sub> catalyst

**Table 1.** Comparison of results obtained by various research groups for naphthalene removal. Temp = operating temperature, Naph = naphthalene.

Plasma	Catalyst	Temp (°C)	Gas mixture	Naph initial concentration (ppm)	SIE (J l <sup>-1</sup> )	NRE (%)	EE (g kWh <sup>-1</sup> )	Ref
Pulsed corona	—	200	CO + CO <sub>2</sub> + H <sub>2</sub> + CH <sub>4</sub> + N <sub>2</sub>	500–700	300	>90	21.4	[3]
Corona	—	25	Air + H <sub>2</sub> O	3	20	70	3.2	[38]
DBD	—	30	N <sub>2</sub> /O <sub>2</sub> mixtures	80	85	90	15.7	[39]
DBD	Glass beads	350	N <sub>2</sub> + H <sub>2</sub> + CO + CO <sub>2</sub>	90	220	60	2.2	[40]
Gliding arc	—	500	N <sub>2</sub> + H <sub>2</sub> O	10000	3600	79	47	[44, 48]
Gliding arc	—	40	Air	265	1660	80	2.2	[45]
Gliding arc	—	>650	CO + CO <sub>2</sub> + H <sub>2</sub> + CH <sub>4</sub> + N <sub>2</sub> + H <sub>2</sub> O + air	44000	360	>70	93.6	[46]
Gliding arc	—	300	N <sub>2</sub> + H <sub>2</sub> O	400	1250	70	2.2	[47]
Positive corona	MnO <sub>2</sub>	25	Air-like mixtures	6	n/a	55	n/a	[52]
Pulsed corona	γ-Al <sub>2</sub> O <sub>3</sub>	300	N <sub>2</sub> + CO <sub>2</sub> + CO	500–700	200	>95	27.9	[53]
DBD	Ni/Al <sub>2</sub> O <sub>3</sub>	250	N <sub>2</sub> + H <sub>2</sub> O	n/a	n/a	n/a	n/a	[54]
DBD	TiO <sub>2</sub>	<150	Ambient air	5000	320	88	207.2	This work

and obtained a decent NRE of 70% at 14kV at ambient temperature, while Nair [53] used pulsed corona discharge in combination with  $\gamma$ -Al<sub>2</sub>O<sub>3</sub> and obtained an NRE of more than 95% at an SIE of more than 200 J l<sup>-1</sup> at 300 °C with an EE of approximately 28 g kWh<sup>-1</sup>. Although his NRE was higher than ours (88% for 320 J l<sup>-1</sup>), we worked with a higher initial concentration and at lower temperature, i.e. in conditions that are less favourable to achieve high NRE. Hubner *et al* [40] used a DBD reactor packed with glass beads without/with char particles and their NRE did not exceed 35% (at 400 J l<sup>-1</sup>) and 60% (at 220 J l<sup>-1</sup>) at 350 °C, respectively. These results are in agreement with ours and show that glass bead packing is less effective compared to metal-supported and metal-oxide catalysts. Other groups investigated naphthalene removal by NTP alone. Pemen *et al* [3] obtained an NRE of more than 90% at 300 J l<sup>-1</sup> and 200 °C with an EE of approximately 21 g kWh<sup>-1</sup>, while Ni *et al* [38] achieved an NRE of approximately 70% at 20 J l<sup>-1</sup> with an EE of approximately 3 g kWh<sup>-1</sup> at ambient temperature. Further, Wu *et al* [39] obtained an NRE of approximately 90% at 85 J l<sup>-1</sup> and 30 °C, but again with a lower initial concentration and a lower EE compared to ours. Finally, Yang *et al* [44], Nunally *et al* [46] and Lim *et al* [48] operated gliding arc discharge at temperatures above 500 °C. They treated high initial concentrations of naphthalene (>10000 ppm) and obtained an NRE of 70%–80%, with EEs of 47 g kWh<sup>-1</sup> [44, 48] and 94 g kWh<sup>-1</sup> [46]. As gliding arc discharge energy consumption is usually quite high, from an economic point of view its use is only favourable if the initial concentration of naphthalene is relatively high, as it was in these studies. If low initial concentrations of naphthalene 265 and 400 ppm were treated by the gliding arc discharge, as in [45, 47], respectively, the EE only reached 2.2 g kWh<sup>-1</sup>. In comparison with the results presented in table 1, our plasma catalytic TiO<sub>2</sub> system showed very high energy efficiency of 207 g kWh<sup>-1</sup>. Although many aspects of the removal process remain to be clarified or improved (e.g. the identification of the by-products and their quantitative analysis), the presented

results clearly demonstrated the potential of plasma catalysis for low temperature tar removal.

#### 4. Conclusion

We investigated the effect of NTP generated by an atmospheric pressure DBD of cylindrical geometry, alone and in combination with various packing materials, including catalysts, on tar removal at a relatively low temperature (below 150 °C). The effects of applied voltage and discharge power and the effect of carrier gas (nitrogen, ambient air, oxygen) on naphthalene removal and the formation of gaseous and solid by-products were studied, along with the effects of packing materials (TiO<sub>2</sub>, Pt/γ-Al<sub>2</sub>O<sub>3</sub>, γ-Al<sub>2</sub>O<sub>3</sub>, glass beads). NRE increased with the increase of the amplitude and frequency of the applied voltage, as well as with the discharge power. In oxygen carrier gas, the NRE reached almost 100% and confirmed the dominant role of reactive oxygen species in processes of naphthalene oxidation. The corresponding EE in oxygen was very high (up to approximately 370 g kWh<sup>-1</sup> in the plasma catalytic TiO<sub>2</sub> reactor). In ambient air, the NRE in the plasma catalytic TiO<sub>2</sub> reactor reached 88% for 320 J l<sup>-1</sup> with the EE of 207 g kWh<sup>-1</sup>, compared to the values of only 40% and 95 g kWh<sup>-1</sup> obtained with the plasma reactor. Moreover, the TiO<sub>2</sub> catalyst showed the highest NRE, and also EE, compared to the other packing materials. The main gaseous by-products of naphthalene decomposition were CO, CO<sub>2</sub>, H<sub>2</sub>O and HCOOH. In the FTIR spectra, several other complex gaseous and solid by-products were identified, including 1,4-naphthoquinone and phthalic anhydride, and traces of maleic anhydride, 1,4-benzoquinone and phthalaldehyde. The NRE and EE we obtained compare well to the results of other groups, even though our initial naphthalene concentration was much higher (5000 ppm) and our operating temperature much lower (below 150 °C), i.e. less favourable for achieving efficient naphthalene removal. Our results proved that the combination of NTP with catalysis is a

very effective method for tar removal that allows for superior removal and energy efficiency when compared to catalytic or NTP treatments alone.

## Acknowledgments

This work was supported by Slovak Research and Development Agency grant APVV-0134-12, Slovak Grant Agency VEGA 1/0419/18 and Comenius University grants UK/319/2017 and UK/373/2018. Special thanks go to Matej Sárený for his computational advice and help.

## ORCID iDs

Richard Cimerman  <https://orcid.org/0000-0001-8854-320X>  
Karol Hensel  <https://orcid.org/0000-0001-6833-681X>

## References

- [1] Ehrlich R 2013 *Renewable Energy* (Boca Raton, FL: CRC)
- [2] Materazzi M 2017 *Clean Energy from Waste* (Berlin: Springer)
- [3] Pemen A J M, Nair S A, Yan K, van Heesch E J M, Ptasiński K J and Drinkenburg A A H 2003 *Plasma Polym.* **8** 209–24
- [4] Anis S and Zainal Z A 2011 *Renew. Sustain. Energy Rev.* **15** 2355–77
- [5] Devi L, Nair S A, Pemen A J M, Yan K, van Heesch E J M, Ptasiński K J and Janssen F J J G 2006 *Biomass and Bioenergy—New Research* (New York: Nova Science) ch 10
- [6] Buchiredy P R, Bricka R M, Rodriguez C and Holmes W 2010 *Energy Fuels* **24** 2707–15
- [7] El-Rub Z A, Bramer E A and Brem G 2004 *Ind. Eng. Chem. Res.* **43** 6911–9
- [8] Shen Y and Yoshikawa K 2013 *Renew. Sustain. Energy Rev.* **21** 371–92
- [9] Kim H-H 2004 *Plasma Process. Polym.* **1** 91–110
- [10] Penetrante B M and Schultheis S E 1993 *Non-Thermal Plasma Techniques for Pollution Control* (Berlin: Springer)
- [11] Vandenbroucke A M, Morent R, De Geiter N and Leys C 2011 *J. Hazard. Mater.* **195** 30–54
- [12] Xiao G, Xu W, Wu R, Ni M, Du C, Gao X, Luo Z and Cen K 2014 *Plasma Chem. Plasma Process.* **34** 1033–65
- [13] Urashima K and Chang J-S 2000 *IEEE Trans. Dielectr. Electr. Insul.* **7** 602–14
- [14] Machala Z, Marode E, Morvová M and Lukáč P 2005 *Plasma Process. Polym.* **2** 152–61
- [15] Machala Z, Morvová M, Marode E and Morva I 2000 *J. Phys. D: Appl. Phys.* **33** 3198–213
- [16] Kogelschatz U 2003 *Plasma Chem. Plasma Process.* **23** 1–46
- [17] Whitehead J C 2010 *Pure Appl. Chem.* **82** 1329–36
- [18] Mizuno A 2013 *Catal. Today* **211** 2–8
- [19] Van Durme J, Dewulf J, Leys C and Van Langenhove H 2008 *Appl. Catal. B* **78** 324–33
- [20] Whitehead J C 2016 *J. Phys. D: Appl. Phys.* **49** 243001
- [21] Mei D, Zhu X, Wu Ch, Ashford B, Williams P T and Tu X 2016 *Appl. Catal. B* **182** 525–32
- [22] Neyts E C, Ostrikov K K, Sunkara M K and Bogaerts A 2015 *Chem. Rev.* **115** 13408–46
- [23] Neyts E C 2016 *Plasma Chem. Plasma Process.* **36** 185–212
- [24] Kim H-H, Teramoto Y, Ogata A, Takagi H and Nanba T 2016 *Plasma Chem. Plasma Process.* **36** 45–72
- [25] Veerapandian S K P, Leys Ch, De Geiter N and Morent R 2017 *Catalysts* **7** 1–33
- [26] Hammer T, Kappes T and Baldauf M 2004 *Catal. Today* **89** 5–14
- [27] Huang Y, Dai S, Feng F, Zhang X, Liu Z and Yan K 2015 *Environ. Sci. Pollut. Res.* **22** 19240–50
- [28] Kim H H, Ogata A and Futamura S 2005 *J. Phys. D: Appl. Phys.* **38** 1292–300
- [29] Delagrange S, Pinard L and Tatibouët J-M 2006 *Appl. Catal. B* **68** 92–8
- [30] Subrahmanyam Ch, Magureanu M, Renken A and Kiwi-Minsker L 2006 *Appl. Catal. B* **65** 150–6
- [31] Nasonova A, Pham H C, Kim D-J and Kim K-S 2010 *Chem. Eng. J.* **156** 557–61
- [32] Kirkpatrick M J, Finney W C and Locke B R 2004 *Catal. Today* **89** 117–26
- [33] Parvulescu V I, Magureanu M and Lukeš P 2012 *Plasma Chemistry and Catalysis in Gases and Liquids* (Weinheim: Wiley)
- [34] Tu X and Whitehead J C 2012 *Appl. Catal. B* **125** 439–48
- [35] Nair S A, Pemen A J M, Yan K, van Heesch E J M, Ptasiński K J and Drinkenburg A A H 2003 *Plasma Chem. Plasma Process.* **23** 665–80
- [36] Nair S A et al 2004 *J. Electrostat.* **61** 117–27
- [37] Bituryn V A, Filimonova E A and Naidis G V 2009 *IEEE Trans. Plasma Sci.* **37** 911–9
- [38] Ni M, Shen X, Gao X, Wu Z, Lu H, Li Z, Luo Z and Cen K 2011 *J. Zhejiang Univ. Sci. A* **12** 71–7
- [39] Wu Z, Wang J, Han J, Yao S, Xu S and Martin P 2016 *IEEE Trans. Plasma Sci.* **45** 154–61
- [40] Hübner M, Brandenburg R, Neubauer Y and Röpcke J 2015 *Contrib. Plasma Phys.* **55** 747–52
- [41] Abdelaziz A A, Seto T, Abdel-Salam M and Otani Y 2014 *Plasma Chem. Plasma Process.* **34** 1371–85
- [42] Chun Y N, Kim S Ch and Yoshikawa K 2012 *Int. J. Environ. Protect.* **2** 1–8
- [43] Liu S, Mei D, Wang L and Tu X 2017 *Chem. Eng. J.* **307** 793–802
- [44] Yang Y Ch and Chun Y N 2011 *Korean J. Chem. Eng.* **28** 539–43
- [45] Yu L, Li X, Tu X, Wang Y, Lu S and Yan J 2010 *J. Phys. Chem. A* **114** 360–8
- [46] Nunnally T, Tsangaris A, Rabinovich A, Nirenberg G, Chernets I and Fridman A 2014 *Int. J. Hydrog. Energy* **39** 11976–89
- [47] Liu S, Mei D, Ma Y and Tu X 2017 Plasma gas cleaning process for the removal of model tar compound from biomass gasification *Poster Presentation at 23rd Int. Symp. on Plasma Chemistry (Montréal)*
- [48] Lim M S and Chun Y N 2012 *Environ. Eng. Res.* **17** 89–94
- [49] Tao K, Ohta N, Liu G, Yoneyama Y, Wang T and Tsubaki N 2013 *Fuel* **104** 53–7
- [50] Liu S Y, Mei D H, Nahil M A, Gadkari S, Gu S, Williams P T and Tu X 2017 *Fuel Process. Technol.* **166** 269–75
- [51] Liu L, Wang Q, Ahmad S, Yang X, Ji M and Sun Y 2017 *J. Energy Inst.* 1–13 (<https://doi.org/10.1016/j.joei.2017.09.003>) at press
- [52] Gao X, Shen X, Wu Z, Luo Z, Ni M and Cen K 2008 *Electrostatic Precipitation* ed K Yan (Berlin: Springer) pp 713–7
- [53] Nair S A 2004 Corona plasma for tar removal *PhD thesis Technische Universiteit Eindhoven*
- [54] Blanquet E, Nahil M A and Williams P T 2017 *Book of Extended Abstracts of 23rd Int. Symp. on Plasma Chemistry (Montréal)* pp 1084–5
- [55] Lee B-Y, Park S-H, Lee S-C, Kang M and Choung S-J 2004 *Catal. Today* **93–5** 769–76
- [56] Kang M, Kim B-J, Cho S M, Chung C-H, Kim B-W, Han G Y and Yoon K J 2002 *J. Mol. Catal. A* **180** 125–32

- [57] Feng X, Liu H, He Ch, Shen Z and Wang T 2018 *Catal. Sci. Technol.* **8** 936–54
- [58] Wallis A E, Whitehead J C and Zhang K 2007 *Catal. Lett.* **113** 29–33
- [59] Guaitella O, Thevenet F, Puzenat E, Guillard C and Rousseau A 2008 *Appl. Catal. B* **80** 296–305
- [60] Pekárek S, Pospíšil M and Krýsa J 2006 *Plasma Process. Polym.* **3** 308–15
- [61] Coll R, Salvado J, Farriol X and Montane D 2001 *Fuel Process. Technol.* **74** 19–31
- [62] Jmróz P, Kordylewski W and Wnukowski M 2018 *Fuel Process. Technol.* **169** 1–14
- [63] Materazzi M, Lettieri P, Mazzei L, Taylor R and Chapman C 2015 *Fuel Process. Technol.* **137** 259–68
- [64] Butterworth T and Allen R W K 2017 *Plasma Sources Sci. Technol.* **26** 065008
- [65] Abdelaziz A A, Seto T, Abdel-Salam M and Otani Y 2013 *J. Hazard. Mater.* **246–7** 26–33
- [66] Janda M, Martišovits V, Hensel K and Machala Z 2016 *Plasma Chem. Plasma Process.* **36** 767–81
- [67] Stancu G D, Kaddouri F, Lacoste D A and Laux C O 2010 *J. Phys. D: Appl. Phys.* **43** 124002
- [68] Socrates G 1994 *IR Characteristic Group Frequencies—Table and Charts* (New York: Wiley)
- [69] Aranda A, López J M, Murillo R, Mastral A M, Dejoz A, Vázquez I, Solsona B, Taylor S H and García T 2009 *J. Hazard. Mater.* **171** 393–9
- [70] Theurich J, Bahnemann D-W, Vogel R, Ehamed F E, Alhakimi G and Rajabres I 1997 *Res. Chem. Intermed.* **23** 247–74
- [71] Pramauro E, Bianco Prevot A, Vincenti M and Gamberini R 1998 *Chemosphere* **36** 1523–42
- [72] Mahmoodi V and Sargolzaei J 2014 *Desalin. Water Treat.* **52** 6664–72
- [73] Mondal K, Bhattacharyya S and Sharma A 2014 *Ind. Eng. Chem. Res.* **53** 18900–9
- [74] Ndifor E N, Garcia T and Taylor S H 2006 *Catal. Lett.* **110** 125–8
- [75] Shie J L, Chang C Y, Chen J H, Tsai W T, Chen Y H, Chiou C S and Chang C F 2005 *Appl. Catal. B* **58** 289–97
- [76] Sellick D R, Morgan D J and Taylor S H 2015 *Catalysts* **5** 690–702
- [77] Yuan M H, Chang C Y, Shie J L, Chang C C, Chen J H and Tsai W T 2010 *J. Hazard. Mater.* **175** 809–15
- [78] Song C and Schmitz D 1999 *Sekiyu Gakkaishi* **42** 287–98
- [79] Wang T J, Chang J, Wu C Z, Fu Y and Chen Y 2005 *Biomass Bioenergy* **28** 508–14
- [80] Kim H H, Kim J H and Ogata A 2009 *J. Phys. D: Appl. Phys.* **42** 135210
- [81] Liotta L F 2010 *Appl. Catal. B* **100** 403–12
- [82] Ray D, Reddy P M K and Challapalli S 2017 *Top. Catal.* **60** 869–78
- [83] Kim S S, Lee H, Na B K and Song H K 2004 *Catal. Today* **89** 193–200